A Developmental Switch of AMPA Receptor Subunits in Neocortical Pyramidal Neurons

Sanjay S. Kumar, Alberto Bacci, Viktor Kharazia, and John R. Huguenard

Department of Neurology and Neurological Sciences, Stanford University Medical Center, Stanford, California 94305-5122

AMPA receptors mediate most of the fast excitatory neurotransmission in the brain, and those lacking the glutamate receptor 2 (GluR2) subunit are Ca^{2+}-permeable and expressed in cortical structures primarily by inhibitory interneurons. Here we report that synaptic AMPA receptors of excitatory layer 5 pyramidal neurons in the rat neocortex are deficient in GluR2 in early development, approximately before postnatal day 16, as evidenced by their inwardly rectifying current–voltage relationship, blockade of AMPA receptor-mediated EPSCs by external and internal polyamines, permeability to Ca^{2+}, and GluR2 immunoreactivity. Overall, these results indicate that neocortical pyramidal neurons undergo a developmental switch in the Ca^{2+} permeability of their AMPA receptors through an alteration of their subunit composition. This has important implications for plasticity and neurotoxicity.

Key words: AMPA receptors; GluR2 subunit; Ca^{2+} permeability; pyramidal neurons; neocortex; developmental switch

Several important aspects of neurotransmitter receptor function rely on the underlying subunit composition. For example, ligand affinity and ion conductance properties such as gating, permeation, and rectification are all affected by alterations in receptor subunits (Hollmann and Heinemann, 1994; Angulo et al., 1997). Channels with differing biophysical properties arise from the combination of distinct subunits, resulting in a surprisingly heterogeneous population of receptor subtypes expressed in unique patterns in the brain. The AMPA class of ionotropic glutamate receptors, which mediate fast excitatory synaptic transmission in the neocortex, are heteromultimeric structures comprised of glutamate receptor subunits 1–4 (GluR1–4) with varying stoichiometries (Hollmann and Heinemann, 1994). AMPA receptors (AMPARs) that lack the GluR2 subunit have traditionally been associated with inhibitory interneurons (McBain and Dingledine, 1993; Jonas et al., 1994; Geiger et al., 1995; Zhou and Hablitz, 1998; Yin et al., 1999) and have been shown to be permeable to Ca^{2+} (Jonas and Burnashev, 1995; Geiger et al., 1995; Gu et al., 1996; Washburn et al., 1997). Whether AMPARs located at excitatory synapses on principal neurons are also permeable to Ca^{2+} remains unknown and may be of importance, given the diverse intracellular effects of Ca^{2+} as a ubiquitous second messenger in development (Aamodt and Constantine-Paton, 1999), synaptic plasticity (Malenka et al., 1989; Jonas and Burnashev, 1995; Jia et al., 1996; Mahanty and Sah, 1998; Rohrbough and Spitzer, 1999; Liu and Cull-Candy, 2000), and excitotoxicity (Prince and Connors, 1984; Swann et al., 1993; Schwartzkroin, 1995).

Using the commissural connections of the corpus callosum as a model system for intracortical (corticocortical) excitation, we tested this hypothesis by examining whether the functional properties of synaptic AMPARs on layer 5 pyramidal neurons changed with respect to the GluR2 subunit during early postnatal development [postnatal day 13 (P13) to P21]. In this report, GluR2 refers to the edited version of the subunit at its Gln/Arg site. Most (>99%) GluR2 (GluRB) subunits expressed in the brain are edited at this position to an Arg residue. Such edited subunits, unlike the unedited (Gln) forms, confer Ca^{2+} impermeability to heteromeric receptors (Hollmann et al., 1991; Burnashev et al., 1992). Changes in subunit composition of these receptors were assayed using known biophysical and pharmacological properties of GluR2-containing and -lacking AMPARs together with immunohistochemistry to estimate overall levels of GluR2 expression in the neurons. Ca^{2+} permeability through these receptors was determined directly at the level of the synapse using ion substitution experiments.

Our results support the conclusion that during early development, synaptic AMPARs on neocortical pyramidal neurons undergo a switch in their functional properties by either altering their subunit composition to incorporate GluR2 or changing their stoichiometry to increase the copy number of the subunit (Washburn et al., 1997) and consequently modifying their Ca^{2+} permeability.

MATERIALS AND METHODS

In vitro *slice preparation and electrophysiology.* Coronal slices (300 μm) were cut from brains of Sprague Dawley rats, ranging in age between P13 and P21, anesthetized with pentobarbital (50 mg/kg). These were prepared with a vibratome in a chilled (4°C) low-Ca^{2+}, low-Na^+ "cutting solution" containing (in mM): 234 sucrose, 11 glucose, 24 $NaHCO_3$, 2.5 KCl, 1.25 NaH_2PO_4, 10 $MgSO_4$, and 0.5 $CaCl_2$ equilibrated with a 95 and 5% mixture of O_2 and CO_2. Slices were allowed to equilibrate in oxygenated artificial CSF (ACSF; in mM: 126 NaCl, 26 $NaHCO_3$, 2.5 KCl, 1.25 NaH_2PO_4, 2 $MgCl_2$, 2 $CaCl_2$, and 10 glucose, pH 7.4) first at 32°C for 1 hr and subsequently at room temperature before being transferred to the recording chamber. Recordings were obtained at 32 ± 1°C from layer 5 pyramidal neurons in the agranular frontal cortex (Paxinos and Watson, 1986), chosen to take advantage of the optimized

Received July 25, 2001; revised Jan. 28, 2002; accepted Jan. 29, 2002.

This work was supported by an American Epilepsy Society research training fellowship (S.S.K.) and by grants from the National Institutes of Health. We thank C. Lin for assistance with immunohistochemistry and R. C. Malenka, R. W. Tsien, S. Hestrin, and D. Porcello for critiquing an early version of this manuscript.

Correspondence should be addressed to Dr. John R. Huguenard at the above address. E-mail: John.Huguenard@Stanford.edu.

intrahemispheric connectivity through the callosum in this region, using a visualized infrared setup such that cell morphology and location within the various cortical lamina could be identified. Recording electrodes (1.2–2 μm tip diameters, 3–6 MΩ) contained (in mM): 120 cesium gluconate, 1 $MgCl_2$, 1 $CaCl_2$, 11 KCl, 10 HEPES, 2 NaATP, 0.3 NaGTP, 1 *N*-(2,6-dimethylphenylcarbamoylmethyl) triethylammonium bromide, 11 EGTA, pH 7.3 (corrected with Cs-OH, 290 mOsm), and 0.05 spermine (in experiments indicated). Slices were maintained in oxygenated (95% O_2 and 5% CO_2) ACSF, and drugs and chemicals were applied through the perfusate (2 ml/min).

Concentric bipolar electrodes (CB-XRC75; Frederick Haer & Co.) with 75 μm tip diameters were positioned on the callosal tract, intracortically in close proximity to the recorded neuron (Fig. 1A), or both, and constant current pulses 50–300 μsec in duration and 100–500 μA in amplitude were applied at low frequencies (0.1–0.3 Hz). Callosal stimulation potentially activates fibers in both orthodromic and antidromic directions, each of which in turn activates monosynaptic excitatory connections onto the recorded pyramidal neuron (Kumar and Huguenard, 2001). Thus, this model consists of activating a well defined, relatively homogeneous population of intracortical excitatory connections. Stimulation parameters were determined by increasing current strength until postsynaptic responses could be evoked and were held constant at ~1.2 times the threshold for obtaining a detectable response throughout the remainder of the experiment (thresholds were characterized by a large proportion of failures; Dobrunz and Stevens, 1997). EPSCs were recorded with an Axopatch-1D amplifier (Axon Instruments, Foster City, CA) and pClamp software (Axon Instruments), filtered at 1–2 kHz, digitized at 10 kHz, and stored on VHS videotapes (Neurocorder DR-484; Neuro Data Instrument Corp.). Series resistance was monitored continuously, and those experiments in which this parameter changed by >20% were rejected. No series resistance compensation was used.

Time constants for PSCs were obtained from single exponential fits of averaged records using Clampfit (Axon Instruments). Traces shown in the figures are averages of 10–20 consecutive responses (at 0.33 Hz), and all values are expressed as mean ± SEM. *I–V* curves were recorded by changing membrane potential according to a predetermined randomized sequence to avoid discrepancies associated with any long-term changes in the responses. Statistical differences were measured using the Student's *t* test unless indicated otherwise. The following compounds were bath applied as required for specific protocols: D(-)-2-amino-5-phosphonopentanoic acid (D-APV), 2,3-dihydro-6-nitro-7-sulfamoyl-benzo(F)quinoxaline (NBQX, diluted in dimethylsulfoxide, <0.1% final concentration), picrotoxin (all from Research Biochemicals/Sigma, St. Louis, MO), and *N*-(4-hydroxyphenylpropanoyl)-spermine trihydrochloride (NHPP-spermine; Tocris Cookson; made fresh on the day of use).

Histology. Cytoplasmic GluR2 levels in pyramidal neurons were estimated under two different conditions: (1) in slices in which pyramidal cells were filled with Biocytin (via the internal solution, 0.05%; Sigma) during electrophysiology and (2) in sections obtained from intact post-fixed brains using an unbiased sample of cells in the corresponding anatomical region. A monoclonal antibody that recognized a tertiary structure of a 256-residue fragment of the N terminus, unique to GluR2 (MAB397, 1:1500; Chemicon, Temecula, CA) was used in both cases. This antibody, previously characterized as 6C4, has been shown not to cross-react with any detectable levels of other AMPA/kainate subunits on Western blots or immunocytochemical tests performed on human embryonic kidney 293 cells that were transfected with corresponding cDNAs (Vissavajjhala et al., 1996). After electrophysiology, slices were fixed overnight in 4% paraformaldehyde in phosphate buffer (PB), pH 7.4, at 4°C before being cut into 40-μm-thick serial sections on a Cryo-Histomat sliding microtome and collected in PB. To obtain an anatomical confirmation of the shape, size, and location of recorded pyramidal neurons, sections were incubated in an avidin–biotin HRP complex (ABC kit, PK-4000; Vector Laboratories, Burlingame, CA), and the peroxidase product was histochemically visualized using diaminobenzidine. Sections containing biocytin-filled neurons were incubated sequentially in 50% ethanol (20 min) and 10% normal donkey serum (in PBS for 30 min to block nonspecific labeling) with an intermittent PBS rinse followed by a final overnight incubation in a mixture of streptavidin-Texas Red conjugate (Vector Laboratories; 1:500) and the primary (anti-GluR2) antibody. This was followed by a 2 hr incubation with secondary donkey anti-mouse antibody tagged with fluorescein (Jackson ImmunoResearch, West Grove, PA; 1:250) on the following day. Sections were mounted on slides using standard histological mounting media and coverslipped for microscopy.

A method of quantification was chosen that minimized errors in the estimation of GluR2 immunoreactivity that might arise from age-dependent variations such as in fixation and antibody binding within different tissues. Each section served as its own control, and data are presented as the difference between averaged immunoreactivities of the biocytin-filled cells and the surrounding neuropil (background) in respective sections (Fig. 2*C,D*).

Changes in coexpression of GluR2 and GluR1(4) subunits (expressed as ratios) were assayed in a population of pyramidal cells from the same cortical region used for electrophysiology in intact brains from four animals aged P12 (two) and P21 (two), respectively. After deep anesthesia (Nembutal, 80 mg/kg), animals were perfused with 4% paraformaldehyde in PB via the aorta (10 min with flushes of saline before and after fixation). Brains were subsequently removed and immersed overnight in 30% sucrose in PB at 4°C until the following day, when frozen sections 40 μm thick were cut using a sliding microtome. Nonadjacent serial sections were processed for double GluR1(4) and GluR2 immunofluorescence using the same procedure for biocytin-filled neurons and GluR2 described above, except for the addition of a polyclonal GluR1 or GluR4 antibody (Chemicon; 1:250 in PBS for GluR1 and 1:500 for GluR4) to the primary mixture. GluR1(4) immunoreactivity was visualized using a 2 hr incubation with biotin-conjugated donkey anti-rabbit IgG (Jackson ImmunoResearch; 1:250 in PBS), followed by incubation with streptavidin-Texas Red conjugate (Vector Laboratories; 1:500 in PBS) for an additional 2 hr. Sections were mounted on slides and coverslipped for microscopy using Vectashield mounting medium.

Double immunofluorescence was assessed with a laser confocal microscope [Molecular Dynamics (Sunnyvale, CA) 2010 for the biocytin study and Bio-Rad (Hercules, CA) Radiance 2000 for GluR2 versus GluR1(4)]. Cross-talk between channels, especially bleed-through of the Texas Red [biocytin or GluR1(4)] signal to the FITC channel (GluR2), was minimized using a bandpass 530 ± 15 nm emission filter for FITC and a long-pass 590 nm filter for the Texas Red channel. Adjacent sections were routinely stained with thionin to reveal cortical lamination (Fig. 1*C*). We assumed that somatic measurements of immunofluorescence are an indicator of overall levels of GluR2 expression within a given neuron. The intensity of immunofluorescence in biocytin-labeled neurons was determined from the averaged gray-scale value (0–255, 8 bit) of 4 measurements within the perikaryon (Fig. 2C_2D_2) using NIH Image software. GluR2/1 or GluR2/4 double immunofluorescence of pyramidal cells in sections from intact brains was obtained using 24 bit red–green–blue images (0.04 mm^2) using SigmaScan software (version 5; SPSS Inc, Chicago, IL).

Ion exchange experiments. High-Ca^{2+} solutions were applied via a local perfusion system that allowed fast exchange of media at the level of the synapse. The perfusion pipette was placed just above the slice and positioned such that the flow through the pipette covered a large portion of the dendritic extent of the cell of interest (see Fig. 5*A*). Sections were maintained in oxygenated (100%) HEPES-buffered ringer comprising (in mM): 135 NaCl, 2.5 KCl, 1 $MgCl_2$, 10 HEPES, and 1.8 $CaCl_2$, pH adjusted with NaOH to 7.4 and osmolarity with sucrose to 290 mOsm to which (in μM): 50 picrotoxin, 40 D-APV, and 0.05 NBQX were added separately. The 1.8 (control), 10, and 30 mM Ca^{2+} solutions were identical in composition to the bathing media except for $CaCl_2$ and NaCl concentrations which varied as (in mM): 1.8 and 135, 10 and 122.7, and 30 and 92.7, respectively. Miniature EPSCs (mEPSCs) were recorded with (in μM): 1 tetrodotoxin (TTX), 50 picrotoxin, and 100 D-APV added to the 1.8 and 10 mM Ca^{2+} solutions. mEPSCs were analyzed using homemade software (Detector; J. R. Huguenard), and the threshold for their detection was set at 3 × root mean square noise level. Reversal potential (E_{rev}) values were estimated from *I–V* relationships by linear interpolation.

Permeability ratios were computed using ionic activities instead of concentrations. Activity coefficients (γ) for various ions were computed according to the methods of Pitzer and Mayorga (1973) and Ammann et al. (1975). The respective γ values estimated for Na^+, K^+, and Ca^{2+} for the different Ca^{2+} solutions were as follows: 1.8 mM Ca^{2+}, 0.75, 0.71, and 0.298; 10 mM Ca^{2+}, 0.74, 0.69, and 0.295; and 30 mM Ca^{2+}, 0.71, 0.68, and 0.289. γ for the internal solution was 0.72. Final ionic activity for solutions was computed as the product of γ and the corresponding molar concentration. The relative permeability of Ca^{2+} with respect to Na^+ was estimated from a nonlinear least squares fit of reversal potential of the AMPAR-mediated component of the EPSC (as a function of Ca^{2+} activity) to the extended constant-field Goldman–Hodgkin–Katz (GHK) equation (Mayer and Westbrook, 1987, their Eqs. 1–2c).

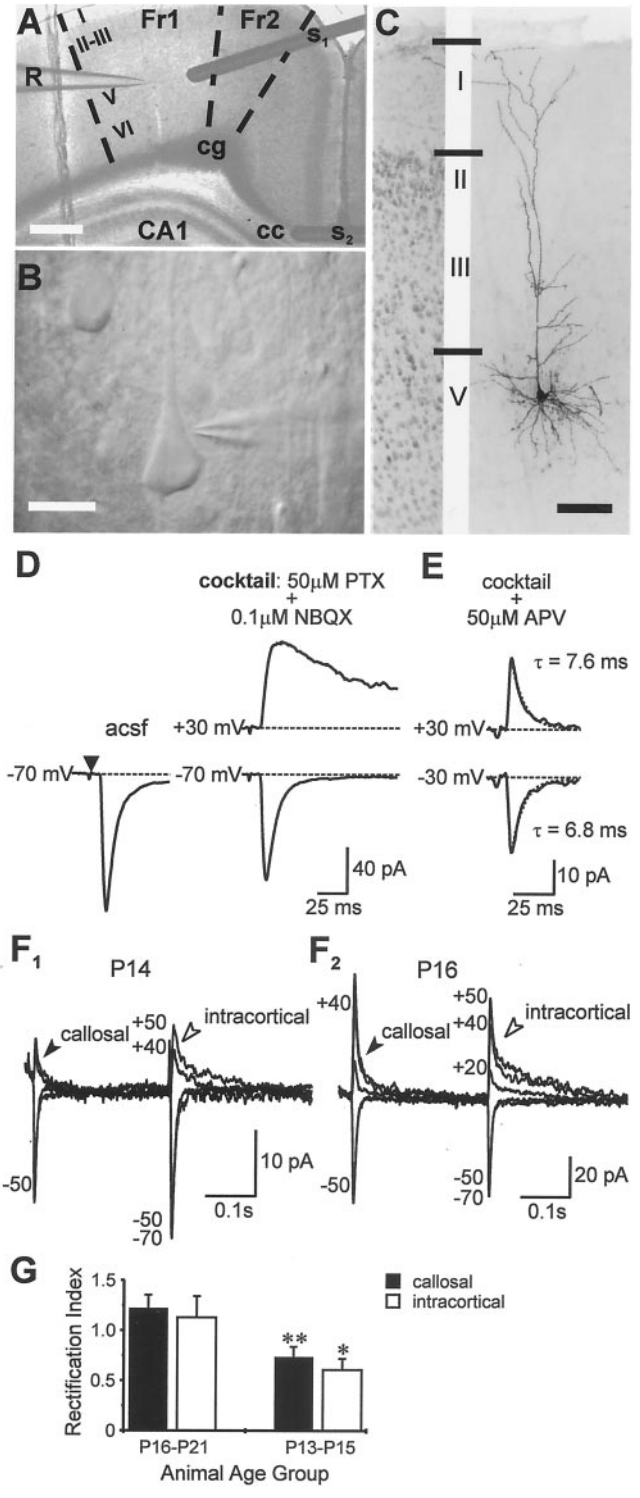

Figure 1. Synaptically activated AMPA currents in pyramidal neurons. *A–E*, Schematic of the model for studying intracortical excitability and properties of pharmacologically isolated monosynaptic EPSCs evoked in pyramidal cells during callosal stimulation. *A*, Cortical slice preparation used in the study showing placement of stimulating (S_1, intracortical; S_2, callosal) and recording (R) electrodes; *Fr1*, *Fr2*, frontal cortex areas 1 and 2; *CA1*, region of hippocampus; *cg*, cingulum; *cc*, corpus callosum (principal commissural pathway linking both cerebral hemispheres). Scale bar, 1 mm. *B*, High-magnification view (Scale bar, 40 μm) depicting the typical morphology of the cells used in electrophysiological recordings. *C*, Photomicrograph of one such cell (P15) filled with biocytin and visualized after fixation with diaminobenzidine (Scale bar, 100 μm) showing extensive arborization of apical and basal dendrites typical of a pyramidal neuron. *C, Left panel*, Portion of the adjacent cortex stained with thionin to reveal cortical lamination. *D, E*, Examples of averaged EPSCs from the same neuron evoked by callosal stimulation (S_2) under the indicated conditions. *PTX*, Picrotoxin. Note that responses were evoked with a fixed latency from stimulus onset (*filled triangle*) and the late, slowly decaying component at +30 mV in *D* was modified by D-APV (*E*) indicating activation of NMDA receptors. Responses in *E* were mediated entirely by AMPA receptors, had identical rise-times at ±30 mV, and were best fit with single exponentials with the indicated time constants. The above approach (*D, E*) was used to isolate the pure AMPAR-mediated component in all subsequent experiments. *F, G*, Rectification of AMPAR-mediated EPSCs is dependent on age but is a property common to synaptic receptors on pyramidal neurons. F_1, F_2, Averages of EPSCs evoked at various holding potentials in the same neurons during concomitant alternate stimulation of the callosum (*filled arrowheads*) and local intracortical excitatory afferents (*open arrowheads*). Peak synaptic currents in P13-P15 neurons (F_1) were generally smaller at positive holding potentials than those at corresponding negative levels, in contrast to P16–P21 neurons (F_2), whose EPSCs had similar amplitudes. Callosally evoked EPSCs showed similar age-dependent rectification as those evoked via intracortical stimulation ($n = 11$). *G*, Rectification indices for the two stimulation paradigms were similar within the respective age groups but differed significantly between age groups. $^*p < 0.05$; $^{**}p < 0.01$.

RESULTS

Isolation of synaptically activated AMPAR currents

Whole-cell voltage-clamp recordings were made from visually identified pyramidal neurons in layer 5 of the agranular frontal cortex close to midline (Fig. 1*A–C*). These cells receive excitatory asymmetric synapses, by way of the corpus callosum, from pyramids located mainly in layer 5 of the homotopic contralateral cortex (Jacobson and Trojanowski, 1974; Ivy and Killackey, 1981; Pandya and Seltzer, 1986; Conti and Manzoni, 1994). Callosal projections are well suited for studying intracortical excitation, because they terminate exclusively on the dendritic spines of pyramidal neurons (Globus and Scheibel, 1967) and are amenable to reliable electrical stimulation (Vogt and Gorman 1982; Kawaguchi, 1992). Near-threshold (Dobrunz and Stevens, 1997) stimulation of the callosum, to activate either a single or a small number of axon collaterals, evoked an inward EPSC in the pyramidal neuron whose peak amplitude averaged 56.5 ± 5.3 pA (n = 31; Fig. 1*D*). EPSCs were isolated in 50 μM picrotoxin and a low concentration (0.1 μM) of the AMPA/kainate receptor antagonist NBQX. The latter was used to prevent hyperexcitability that could arise from the complete blockade of $GABA_A$-mediated inhibition in the tissue. Inclusion of NBQX in the perfusate reduced the peak synaptic current by ~20%. Cesium ions in the internal solution of the recording electrode blocked any K^+ currents mediated through postsynaptic $GABA_B$ receptor activation.

EPSCs were deemed monosynaptic by virtue of their fixed latency from stimulus onset (averaged duration between stimulus and response onsets, 6.1 ± 0.2 msec; n = 30) and their ability to follow stimulus trains (1–20 Hz) without changes in their kinetic properties (Kumar and Huguenard, 2001). At positive holding potentials (+30 mV), an outward, late, and slowly decaying component of the EPSC was revealed. Addition of D-APV (50 μM) to the bathing medium abolished this late component, thereby confirming the presence of NMDA receptors at these synapses (Fig. 1*E*). The pharmacologically isolated, AMPA/kainate receptor-mediated component averaged 28.9 ± 4.4 pA (n = 32) in amplitude at −70 mV and had a 10–90% rise time of 2.3 ± 0.2 msec (see Discussion) and a decay time constant (τ_D) of 6.8 ± 0.5 msec.

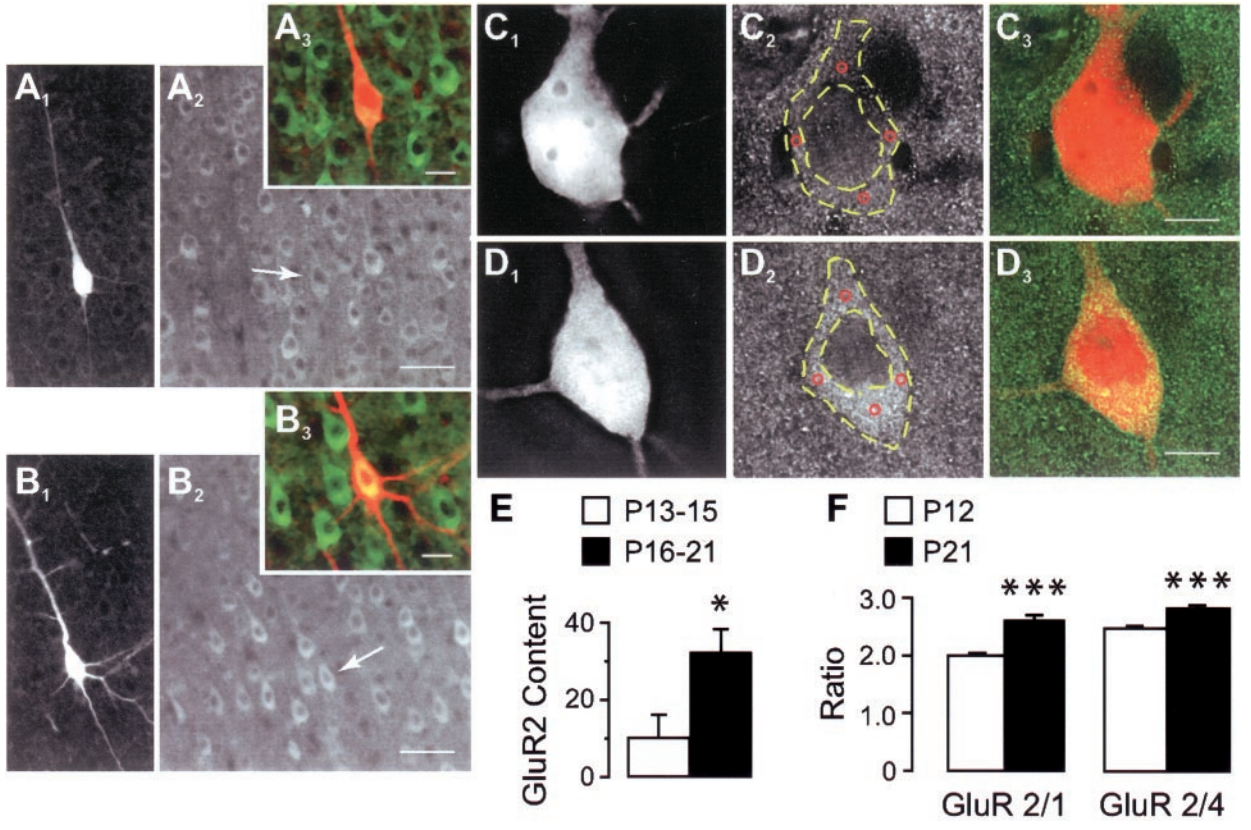

Figure 2. GluR2 expression in pyramidal neurons at different ages. *A, B*, Dual-channel images of recorded biocytin-filled layer 5 pyramidal neurons from P14 (A_1–A_3) and P18 (B_1–B_3) animals immunostained with the GluR2 antibody (A_1, B_1, biocytin-Texas Red; A_2, B_2, GluR2-FITC; A_3, B_3, color overlap). Note that pyramidal neurons, including biocytin-filled cells (A_2, B_2, *arrows*), in the older age group show higher levels of GluR2 immunofluorescence compared with younger under similar conditions of illumination. Scale bars: A_1, A_2, B_1, B_2, 50 μm; A_3, B_3, 20 μm. *C, D*, High-magnification images of young (C_1–C_3) and old (D_1–D_3) biocytin-filled neurons showing that although the intracellular level of GluR2-FITC fluorescence in the young animal (C_2) is comparable with adjacent neuropil and with the intranuclear staining, it is markedly more intense in the corresponding regions of the older neuron (C_2 vs D_2). Note the absence of cross-talk between Texas Red (C_1, D_1) and FITC (C_2, D_2) channels. Immunofluorescence was measured at four locations (C_2 and D_2, *red circles*) within the perikaryon (outlined with *dashed yellow lines*), and the average of these values was used to represent cell brightness (see Materials and Methods). Scale bars, 10 μm. *E*, GluR2 levels in P13-P15 ($n = 6$) and P16-P21 ($n = 9$) biocytin-filled pyramidal neurons based on perikaryon immunofluorescence measurements compared with background as outlined in *C, D*. *F*, Changes in GluR2 immunoreactivity relative to coexpressed GluR1 (or 4) measured separately in a population of layer 5 pyramidal cells from corresponding cortical regions in intact brain sections of animals at the indicated ages (P12, $n = 142$ cells, 11 sections; P21, $n = 83$ cells, 10 sections). $^*p < 0.05$; $^{***}p < 0.0001$.

Rise times (2.7 ± 3.3 msec) and τ_D values (7.2 ± 0.5 msec) at positive holding potentials (+40 to +60 mV) were similar to those isolated at −70 mV ($p > 0.1$; $n = 16$), and all responses could be completely blocked with 10 μM NBQX (data not shown; see Fig. 5*B*). Kainate receptor-mediated responses have been distinguished from those based on AMPARs by their characteristically long decay times at hyperpolarized holding potentials. The comparatively short τ_D for EPSCs isolated in this study, together with the knowledge that expression of kainate receptors in the neocortex is substantially reduced after P7 (Bahn et al., 1994; Kidd and Isaac, 1999), suggests that these were mediated predominantly by the AMPA class of glutamate receptors.

Rectification of AMPAR responses in immature cortex

In pyramidal neurons of animals P16 or older, AMPAR-mediated EPSCs evoked by callosal stimulation were similar in magnitude at equipotential levels on either side of the reversal potential (0 mV), a finding consistent with previous observations (Jonas et al., 1994; Geiger et al., 1995). Surprisingly, however, when recorded in pyramidal neurons from P13–P15 animals, AMPAR-mediated synaptic currents were consistently smaller at positive holding potentials compared with those at corresponding negative levels. The rectification index (RI), defined as the ratio of AMPA conductances measured at +40 and −70 mV, was significantly smaller for P13–P15 neurons (0.7 ± 0.11; $n = 12$; range, 0.3–1.6) than for P16–P21 neurons (1.2 ± 0.13; $n = 11$; range, 0.6–1.8; $p < 0.01$).

To determine whether inward rectification in immature neurons was a cell- or synapse-specific property, i.e., whether it applied specifically to AMPARs located at callosal synapses or more generally to synaptic AMPARs expressed throughout the pyramidal neuron, we compared the callosally evoked AMPAR-mediated EPSCs with those evoked during nonspecific activation of excitatory afferents by a second stimulating electrode placed in close proximity (either on or off column) to the recording electrode (Fig. 1*A*). Synaptic AMPA currents evoked by cortical stimulation were similar to those evoked by callosal stimulation in terms of 10–90% rise times (2.3 ± 0.3 vs 2.3 ± 0.2 msec at −70 mV and 2.34 ± 0.3 vs 2.7 ± 3.3 msec between +40 and +60 mV) and τ_D values (7.1 ± 0.5 vs 6.8 ± 0.5 msec at −70 mV) but had different onset latencies (3.1 ± 0.2 vs 6.1 ± 0.2 msec at −70 mV; $n = 14$; $p < 0.001$). Cortically evoked EPSCs showed similar age-dependent rectification ($RI_{(P13–P15)} = 0.61 \pm 0.11$; $n = 6$; range, 0.4–1.1; Fig. 1F_1; $RI_{(P16–P21)} = 1.13 \pm 0.21$; $n = 10$; range,

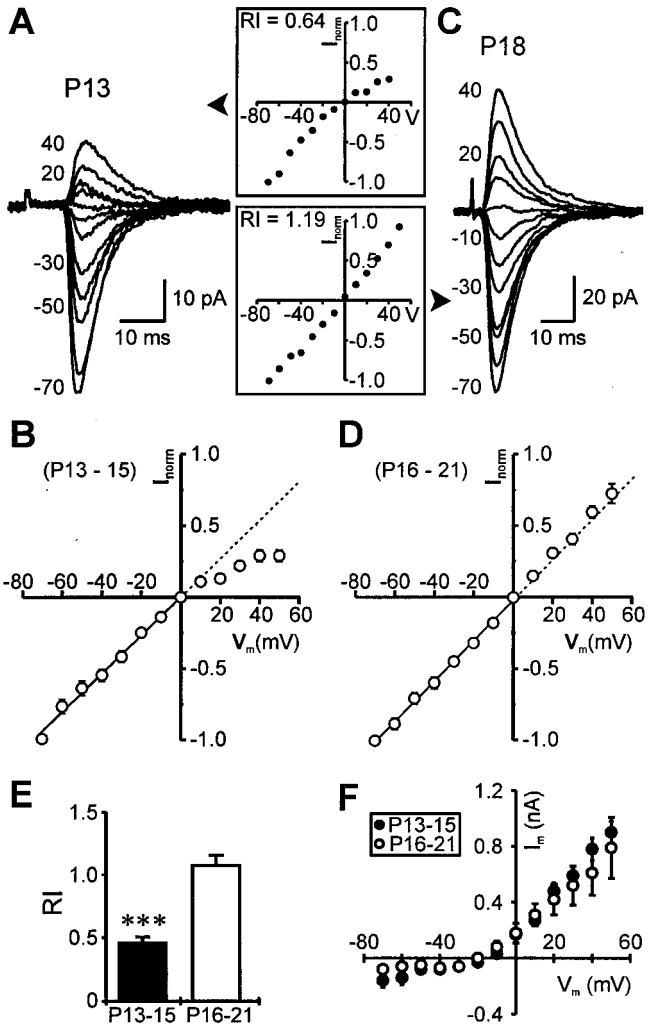

Figure 3. Inclusion of NHPP-spermine (50 μM) in the pipette does not alter age-dependent differences in *I–V* characteristics of AMPAR-mediated EPSCs. *A*, Superimposed averaged records of synaptic currents evoked in a P13 neuron at various holding potentials (−70 to +40 mV; step size, 10 mV; isolated in cocktail solution and 50 μM D-APV) with the polyamine included in the patch pipette. The corresponding *I–V* curve, normalized to the EPSC amplitude at −70 mV, is shown in the *inset*. *B*, Normalized *I–V* relationship of the pooled data taken from P13–P15 neurons showing inward rectification of the EPSCs. Each *point* on the plot (*open circle*) represents an ensemble average of 14 experiments, and error bars indicate SEM where this is greater than the size of the symbol. The *dashed line* is an extension of the linear regression fit of data points at negative holding potentials. *C, D*, In contrast with *A*, *B*, EPSCs recorded from neurons in an older animal were nonrectifying (*C*), and the composite *I–V* profile, averaged from eight P16–P21 neurons, was linear throughout the entire voltage-range (*D*). *E, F*, RIs for the two age groups and averaged holding currents recorded at various membrane potentials in these experiments, respectively. $^{***}p < 0.0001$.

0.5–2.3; Fig. 1F_2) as those evoked by stimulation of the callosum ($RI_{(P13–P15)} = 0.7 \pm 0.11$; $RI_{(P16–P21)} = 1.2 \pm 0.13$; Fig. 1*G*). Although rectification indices of P13–P15 neurons were significantly smaller than those of P16–P21 neurons for both stimulus paradigms ($p < 0.05$ intracortical; $p < 0.01$ callosal), there was no difference between callosal or intracortical stimulation with respect to the RIs for either age group ($p > 0.6$). Additionally, it made no difference whether the stimulating electrode was placed on or off column with reference to the recorded neuron. These results suggest that at two distinct developmental stages, P13–P15 and P16–P21, synaptic AMPARs expressed by the pyramidal neurons share a similar degree of rectification. Further support for a lack of input specificity derives from the finding that spontaneous AMPAR-mediated currents, which presumably arise from activation of multiple inputs onto the recorded pyramidal neurons, displayed age-dependent rectification similar to that of the evoked responses (Kumar and Huguenard, 2001).

Thus immature AMPAR-dependent synapses on pyramidal neurons in general are characterized by inward rectification, in contrast to mature synapses. Because inward rectification is an attribute of AMPARs lacking the GluR2 subunit (Jonas et al., 1994; Geiger et al., 1995; Jonas and Burnashev, 1995; Washburn et al., 1997), we next assayed GluR2 content via immunocytochemistry to test whether pyramidal neurons might alter their expression of GluR2 during development.

Developmental changes in GluR2 immunoreactivity in layer 5 pyramidal neurons

We used double immunofluorescence confocal microscopy to assess GluR2 levels in recorded neurons from each age group. The overall pattern of GluR2 staining in neocortex was similar to that reported previously (Vissavajjhala et al., 1996), revealing a laminar distribution with numerous GluR2-positive pyramidal cells in layers 3 and 5. GluR2 immunoreactivity in recorded biocytin-filled pyramidal neurons (P14; Fig. 2A_1; P18; Fig. 2B_1) was comparable with that detected in neighboring cells in the microscopic field at both ages (Fig. 2A_2,B_2). However, we found that older neurons consistently expressed higher GluR2 immunoreactivity than younger neurons. Representative differences in GluR2 immunofluorescence in these age groups can be seen from overlapped images in Figure 2, A_3, B_3, C_3, and D_3. Consistent with these qualitative observations, GluR2 content, measured in terms of somatic immunoreactivity compared with background (Fig. 2*C–D*; see Histology in Materials and Methods), was significantly lower in P13–P15 biocytin-filled pyramidal neurons than in the P16–P21 cells (9.7 ± 6.5 vs 32.1 ± 6.3 gray-scale units; $n = 6$ and 9, respectively; $p < 0.05$; Fig. 2*E*). Although these immunostaining results do not directly demonstrate changes in synaptic GluR2 expression, they do show that this subunit is developmentally regulated in the same layer 5 pyramidal neurons in which functional changes in synaptic AMPA responses occur.

To rule out the possibility that the developmental increase in GluR2 immunoreactivity might simply be a reflection of an overall increased expression of AMPARs, we simultaneously assayed the coexpression of other subunits (either GluR1 or GluR4) in a population of layer 5 pyramidal neurons from corresponding cortical regions. The ratio of the averaged intensities for GluR2 and GluR1 immunofluorescence was 2.0 ± 0.03 ($n = 142$ cells, 11 sections, two animals) for P12 animals compared with 2.6 ± 0.1 ($n = 83$ cells, 10 sections, two animals) for P21 animals, corresponding to a ~30% increase in the GluR2/GluR1 ratio between these ages ($p < 0.0001$; *t* test; Fig. 2*F*). In comparison, there was also an increase in the separately determined GluR2/GluR4 ratio (~14%) at the corresponding ages (P12, 2.5 ± 0.04; $n = 113$ cells, eight sections; P21, 2.8 ± 0.05; $n = 80$ cell, eight sections; $p < 0.0001$; Fig. 2*F*). These data suggest that GluR2 levels in pyramidal cells are developmentally upregulated relative to both GluR1 and GluR4, warranting further functional assays to determine whether these alterations in relative GluR2 expression are reflected in AMPAR composition at the synaptic level.

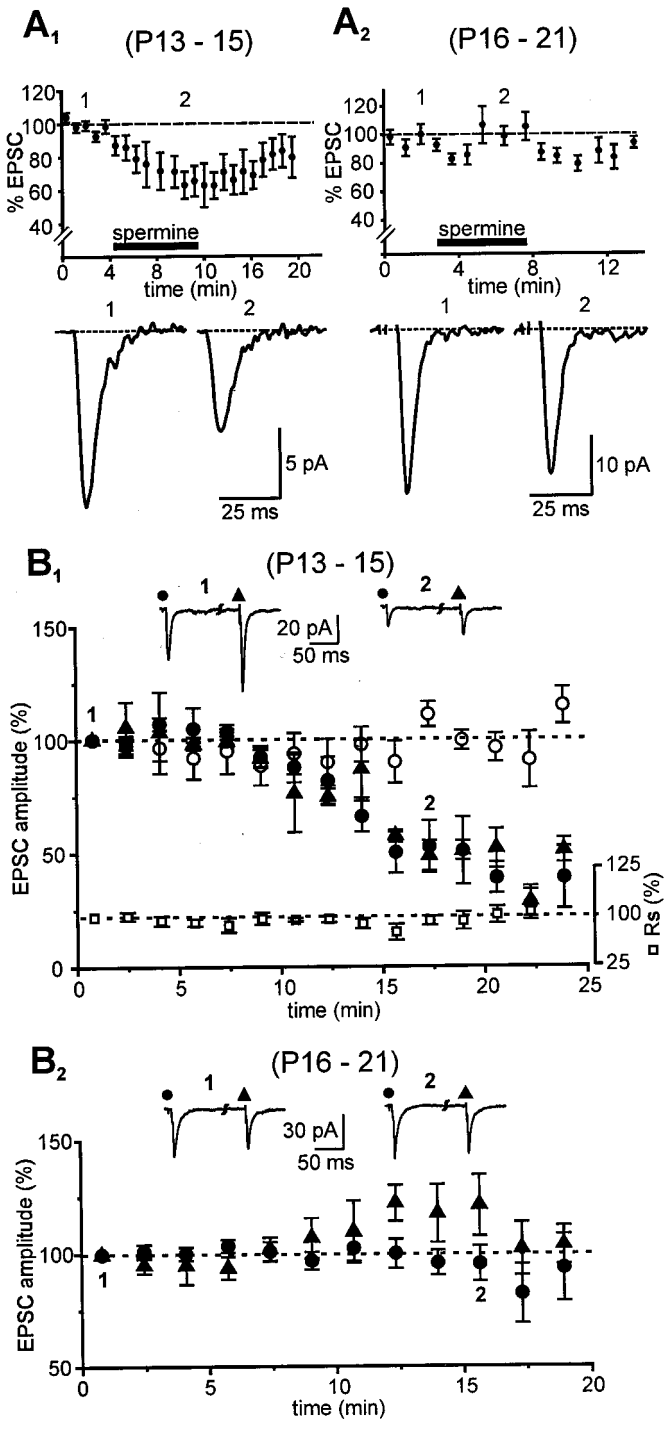

Figure 4. Effects of extracellular (*A*) and intracellular (*B*) polyamine on EPSC amplitude. A_1, A_2, Pooled data ($n = 7$) showing the time course of changes in response amplitudes (percentage of control, −70 mV) of neurons in different age groups in the presence of 5 μM NHPP-spermine applied externally at the times indicated (*black bar*; 100% = average of all control values). EPSCs in A_1 were blocked by 37.1 ± 8.1% as opposed to 1.8 ± 4.6% in A_2 (values correspond to the second designated time point in A_1, A_2, respectively). *Traces* recorded at the times indicated are shown below their respective time plots. EPSCs in all these experiments were isolated in a cocktail and D-APV. B_1, B_2, Inclusion of NHPP-spermine (50 μM) in the patch solution had differential effects on EPSCs depending on the developmental age of the animal. Changes in EPSC amplitude after break-in ($t = 0$ min; holding potential, −70 mV, ACSF) from neurons in the younger (B_1; $n = 6$) and older (B_2; $n = 7$) age groups under different experimental conditions are shown. NHPP-spermine reduced the amplitude of evoked responses during both callosal (●) and intracortical (▲) stimulation in the younger (B_1) but not in the older (B_2) age group. Callosal EPSCs recorded with polyamine-containing patch electrodes were significantly smaller compared with those with control solution (○). Each *point* on the plot represents an ensemble average of the EPSC amplitudes, and error bars indicate SEM. Responses are normalized to the averaged EPSC at $t = 0$ min (100%). Series resistance (□) in these experiments was constant, as shown in B_1. *Traces* at the *top* of the plots are averaged sample records obtained at the times indicated.

Internal polyamines sustain age-related differences in rectification properties

Although rectification properties of AMPAR-mediated EPSCs have commonly been used to indicate Ca^{2+} permeability and GluR2 stoichiometry, several studies have suggested that inward rectification of AMPARs also depends on endogenous spermine (a cytoplasmic polyamine) and that this property is lost under conditions in which polyamines were dialyzed. Conversely, the loss of rectification could be prevented by the inclusion of spermine in the pipette (Donevan and Rogawski, 1995; Isa et al., 1995; Kamboj et al., 1995).

To examine a potential role of intracellular polyamines in the rectification of AMPAR-dependent EPSCs reported here, we obtained their *I–V* relationships in recordings with 50 μM NHPP-spermine (a polyamine with known intracellular effects on AMPAR-mediated responses; Bahring et al., 1997) included in the pipette. EPSCs recorded in this series from pyramidal neurons of P13–P15 animals showed consistent inward rectification (Fig. 3*A*). This was noted by a significant deviation from the linear *I–V* slope obtained from inward responses at negative holding potentials ($n = 14$ neurons; Fig. 3*B*). EPSCs had a reversal potential near 0 mV and, as indicated before, could be completely blocked by NBQX. In contrast, EPSCs recorded from P16–P21 neurons were nonrectifying (Fig. 3*C*), and the composite *I–V* relationship from eight neurons was slightly outwardly rectifying (Fig. 3*D*). The rectification index for P13–P15 neurons was significantly smaller than that for P16–P21 neurons (0.46 ± 0.05 vs 1.08 ± 0.08; $p < 0.0001$; Fig. 3*E*). *I–V* relationships were recorded ~15 min after break-in to allow sufficient time for diffusion of the polyamine, and measurements were made from averages of 20 responses evoked by either callosal or intracortical stimulation. Series resistance was monitored periodically, and the holding currents at various membrane potentials were similar for neurons from the different age groups ($p > 0.5$, paired t test; Fig. 3*F*), suggesting minimal contribution of voltage-clamp errors to the observed differences in rectification.

The rectification index in younger neurons was smaller with spermine in the pipette than without the polyamine (0.46 ± 0.05 vs 0.7 ± 0.11); however, the difference was not statistically significant ($p = 0.08$) because of the greater variability in RI when spermine was omitted (range without spermine, 0.3–1.6; range with spermine, 0.09–0.9). These data are consistent with the notion that inclusion of spermine in the pipette can prevent loss of rectification and do not support the hypothesis that variations in levels of endogenous polyamines can account for the differences in rectification properties observed between the two age groups.

Selective blockade of AMPAR-mediated EPSCs by polyamines in immature neurons

AMPARs devoid of GluR2 are unique not only in their rectification but also in their selective blockade by both external and

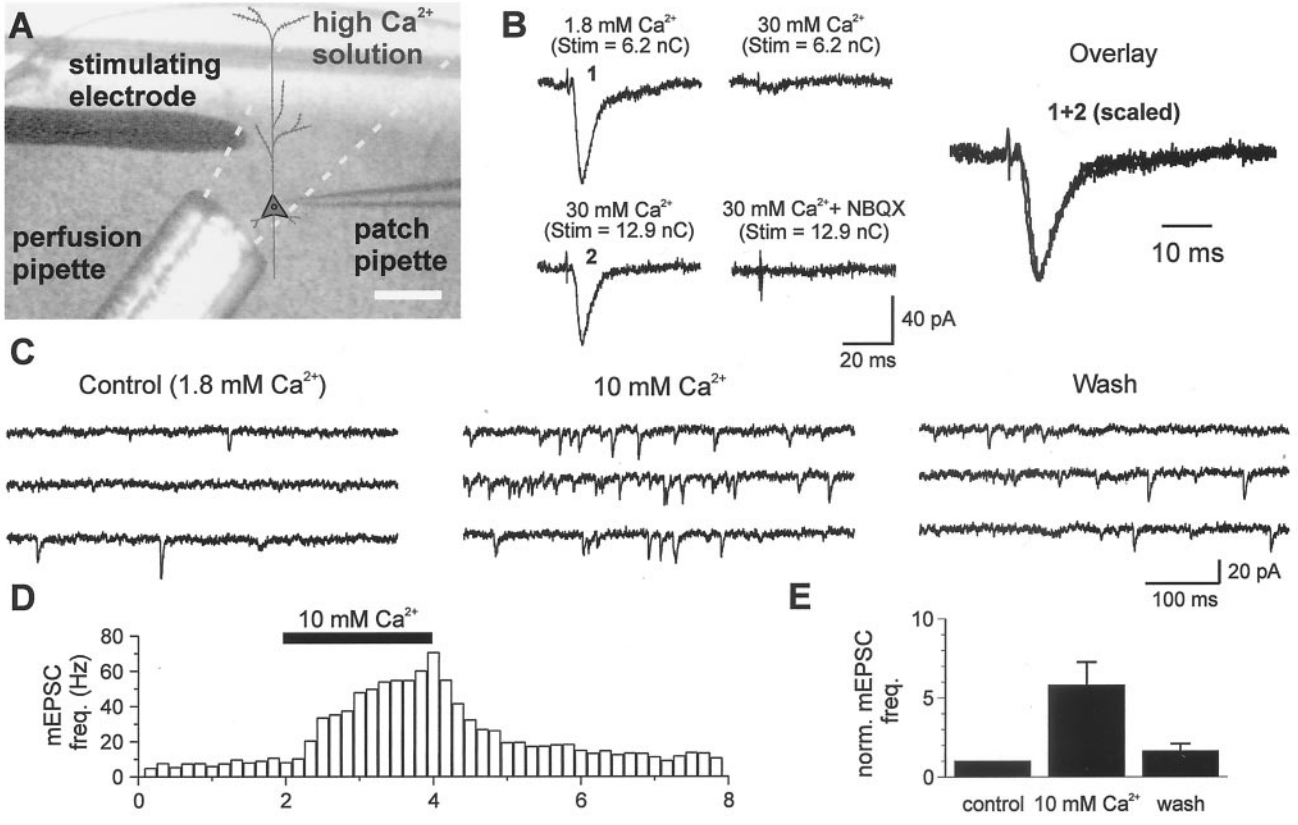

Figure 5. Experimental design and validation of the procedure used to determine Ca^{2+} permeability of synaptic AMPARs. *A*, Schematic of the experimental configuration showing relative placements of the intracortical stimulating electrode and local perfusion pipette with respect to the patch recording electrode. *B*, Representative traces of AMPAR-mediated responses (−70 mV) during perfusion of solutions with different Ca^{2+} concentrations. *Traces* shown are from a P18 animal. Note that it required higher stimulus intensities to evoke EPSCs in high Ca^{2+}. The averaged (percent) increments in charge required to elicit responses when $[Ca^{2+}]_o$ was sequentially elevated from 1.8 to 10 and from 10 to 30 mM were 60.9 and 20.8%, respectively, for P13–P15 neurons and 70.9 and 41.9%, respectively, for P16–P21 neurons. Inclusion of 10 μM NBQX in the local perfusate blocked all EPSCs evoked in high Ca^{2+}. The *numbered* responses in *B* are overlaid such that the second response is scaled to match the amplitude of the first response. Note the fixed latency from stimulus onset for the two responses and the similarity in the shape of the waveforms. *C, D*, mEPSC frequency is increased after local elevation of $[Ca^{2+}]_o$ via the local perfusion system. *C*, Representative traces of mEPSCs recorded from a P19 layer 5 pyramidal neuron in the presence of 1 μM TTX, 50 μM picrotoxin, and 100 μM APV under the indicated conditions. *D*, Time course of changes taken from a different neuron showing the fast onset and offset of the altered mEPSC frequency. *E*, Bar plot of the averaged mEPSC frequency under different $[Ca^{2+}]_o$ conditions ($n = 8$ and 5 cells for *10 mM Ca^{2+}* and *wash*, respectively) normalized to the mean value in *control*. $^*p < 0.05$.

internal polyamines (Bowie and Mayer, 1995; Washburn and Dingledine, 1996; Washburn et al., 1997), although this has not been directly established for synaptic responses. Sensitivity to extracellular polyamines was tested by bath application of NHPP-spermine (5 μM). AMPAR-mediated EPSCs (recorded with polyamine-free patch pipettes) in the P13–P15 neurons were reversibly blocked by 37.1 ± 8.1%, ($n = 7$; $p < 0.005$; measured in Fig. 4A_1, *point 2*), whereas those in the P16–P21 age group were unaffected (1.8 ± 4.6% blockade; $n = 7$; Fig. 4A_2). The differential blockade by NHPP-spermine seen in these experiments was robust and provides further support for a low level of GluR2 expression at synapses of pyramidal neurons in the younger animals. As a further test of the relative deficiency of GluR2 in AMPARs in P13–P15 neurons, we also examined the intracellular effects of 50 μM NHPP-spermine on EPSC amplitude by including it in the patch solution.

Internal polyamines have been shown previously both to prevent the loss of rectification and to reduce the amplitude of GluR2-deficient AMPAR-mediated EPSCs (Donevan and Rogawski, 1995; Kamboj et al., 1995; Koh et al., 1995). Intracellular NHPP-spermine produced a time-dependent reduction of both callosal and intracortically evoked EPSCs in P13–P15 neurons ($p < 0.01$, repeated measures ANOVA; Fig. 4B_1), consistent with passive diffusion of the polyamine from the recording pipette to the activated synapses. The relative block stabilized by ~20 min, at which time callosal and intracortical EPSC amplitudes averaged 53 ± 11.5% ($n = 6$) and 47 ± 9.4% ($n = 3$), respectively, of their values at break-in ($t = 0$ min). Series resistance remained unaltered during the recording sessions, as did callosal responses from sequential recording in neighboring pyramidal neurons in the same sections obtained with polyamine-free patch electrodes. By contrast, in P16–P21 neurons, neither callosal (96 ± 7.8%; $n = 7$) nor intracortical (121 ± 13.5%; $n = 4$) EPSCs were reduced by intracellular NHPP-spermine ($p > 0.4$, repeated measures ANOVA; Fig. 4B_2). The selective reductions in EPSC amplitude in P13–P15 but not P16–P21 neurons provides direct additional evidence for age-specific, GluR2-mediated differences in the subunit composition of synaptic AMPARs.

Differences in Ca^{2+} permeability of AMPARs in synapses

Previous studies have successfully used outside-out patches, isolated from the cell soma, to demonstrate Ca^{2+} permeability through AMPARs deficient in the GluR2 subunit (Jonas and Sakmann, 1992; Jonas et al., 1994; Otis et al., 1995; Itazawa et al., 1997). However, somatic AMPARs on excitatory neurons in the neocortex are primarily extrasynaptic and might have a different complement of subunits compared with the ones located at the synapse (Lerma et al., 1994; Carder, 1997; Yin et al., 1999; Kumar and Huguenard, 2001). To directly investigate Ca^{2+} permeability through these synaptic receptors, we measured the shift in E_{rev} of synaptically activated currents during local perfusion of solutions with different extracellular calcium concentrations (Fig. 5*A*; see Ion exchange experiments in Materials and Methods). Unlike rectification, Ca^{2+} permeability of AMPARs is independent of intracellular polyamines (Gilbertson et al., 1991; Jonas et al., 1994; Kamboj et al., 1995; Otis et al., 1995). Thus this series of experiments was performed without spermine in the patch pipette, and the resultant *I–V* curves in P13–P15 neurons were not expected to display prominent rectification.

We first verified that the extracellular Ca^{2+} concentration could be effectively controlled by our local perfusion system. Evidence for successful solution change included the following: (1) Elevation of $[Ca^{2+}]_o$ reduced the synaptic response amplitude and increased its activation threshold (Fig. 5*B*; cf. Otis et al., 1995), consistent with alteration in both presynaptic and postsynaptic excitability. [Similarities in latency, rise time and decay between the waveforms suggest that the same or similar synapses are activated by the increased stimulus intensity in elevated $[Ca^{2+}]_o$ (Fig. 5*B*, *Overlay*).] (2) Ten micromolar NBQX in the local perfusate completely blocked the synaptic responses, indicating that the local perfusion system effectively alters the extracellular environment at the synapse (Fig. 5*B*). (3) mEPSCs (recorded in the presence of TTX in both age groups) showed a robust and reversible increase in frequency when $[Ca^{2+}]_o$ was altered in the local environment of the recorded neurons (Fig. 5*C–E*). The time course of change in mEPSC frequency (Fig. 5*D*) shows the rapid onset and offset of the Ca^{2+} exchange. A reversible sixfold increase in mEPSC frequency was induced when $[Ca^{2+}]_o$ was raised from 1.8 (control) to 10 mM ($n = 8$; $p < 0.05$, paired *t* test). This result is consistent with an increase in release probability as expected for elevated $[Ca^{2+}]_o$ at the level of the synapse. These data suggest that the local perfusion technique can effectively control extracellular environment in general, and $[Ca^{2+}]_o$ in particular, at the synapse.

I–V relationships for synaptic AMPAR responses in pyramidal neurons of both age groups were obtained under various $[Ca^{2+}]_o$ [1.8 (normal), 10, and 30 mM]. The E_{rev} in 1.8 mM $[Ca^{2+}]_o$ for P13–P15 neurons ($n = 11$) was similar to the value obtained with P16–P21 neurons ($n = 6$; -4.8 ± 2.4 vs -7.4 ± 3.3 mV). When $[Ca^{2+}]_o$ was increased to 10 mM and subsequently to 30 mM, E_{rev} shifted slightly in a positive direction to -3.2 ± 2.2 and 0.1 ± 1.6 mV, respectively, in P13–P15 neurons (Fig. 6*A,C1*). In contrast, E_{rev} shifted in the opposite direction to -13.7 ± 3.2 and -30.4 ± 3.3 mV in the older P16–P21 neurons (Fig. 6*B,C2*), suggesting relative impermeance of the receptors to Ca^{2+}. The differences in E_{rev} were statistically significant between the two age groups ($p < 0.02$ and 0.005 for 10 and 30 mM Ca^{2+}, respectively; Fig. 6*D*) and among the different $[Ca^{2+}]_o$ for the P16–P21 but not P13–P15 neurons ($p < 0.0005$, repeated measures ANOVA).

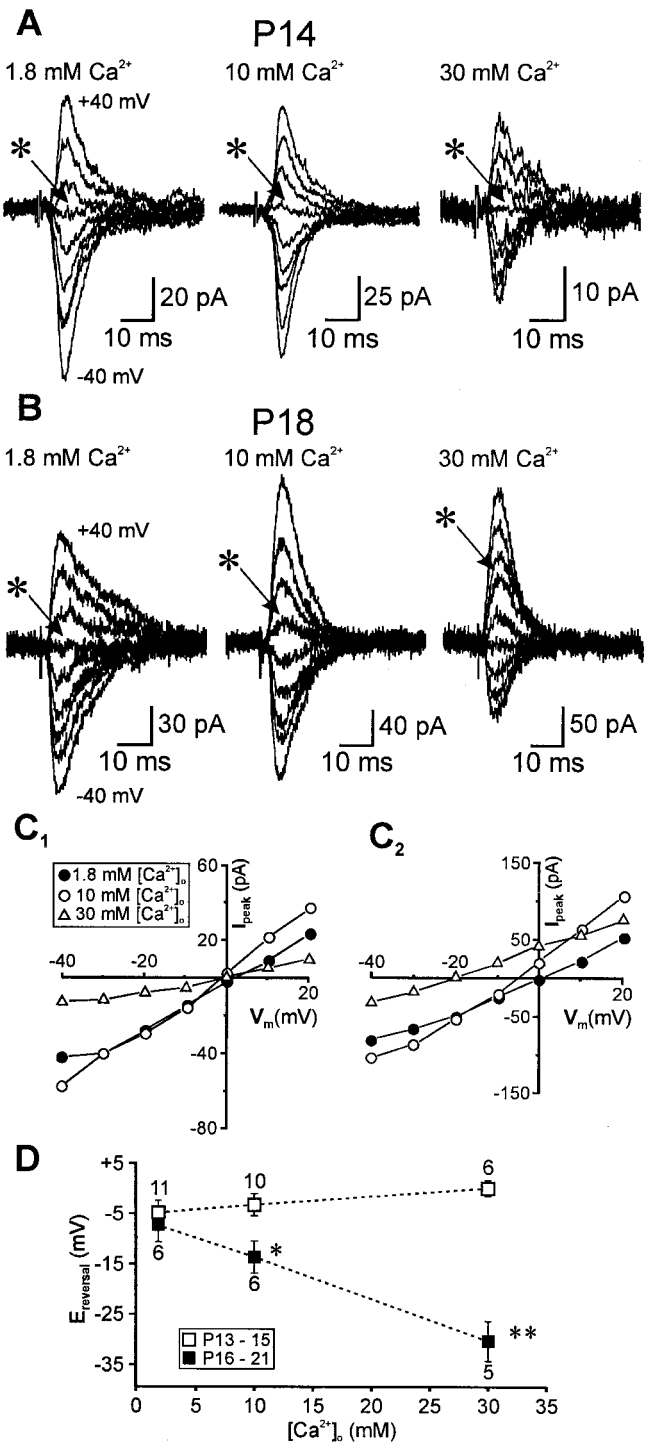

Figure 6. Differential Ca^{2+} permeability of synaptic AMPARs within the identified age groups. *A–C*, Families of representative traces (*A, B*, ±40 mV; step size, 10 mV) and their corresponding *I–V* relationships (C_1, C_2) recorded from animals in the two age groups under various $[Ca^{2+}]_o$ conditions. The *asterisks* in *A* indicate the response at a holding potential of 0 mV. *D*, Plot of the E_{rev} values, measured from *I–V* relationships, as a function of $[Ca^{2+}]_o$. Each *point* represents the mean of the indicated number of experiments in the respective age groups. Note the leftward shift in E_{rev} for the older animals in contrast with the opposite trend (*dashed lines*) observed in the younger animals. Statistical comparisons are between the reversal potentials for animals in the two age groups. $^*p < 0.02$; $^{**}p < 0.005$.

Thus, synaptic AMPAR from only the younger age group displayed significant Ca^{2+} permeability. Using the extended GHK constant-field equation (Mayer and Westbrook, 1987), we estimate that the lack of shift in E_{rev} as a function of Ca^{2+} ionic activities in the younger neurons reflects a Ca^{2+} to Na^{+} permeability ratio (P_{Ca}/P_{Na}) of >2.0 ($n = 11$) compared with a P_{Ca}/P_{Na} ratio of <0.1 ($n = 6$) for the older neurons recorded under the same experimental conditions.

DISCUSSION

Maturation of neocortical circuitry relies in large measure on developmentally regulated changes in its presynaptic and postsynaptic elements. Only recently have we begun to understand the underlying cellular mechanisms responsible for these changes and their potential consequences. GluR2-deficient AMPARs exhibiting inward rectification and a polyamine-dependent block have been described in other brain structures (McBain and Dingledine, 1993; Mahanty and Sah, 1998; Yin et al., 1999) and have been proposed to reside predominantly on inhibitory GABAergic interneurons (McBain and Dingledine, 1993; Jonas et al., 1994; Geiger et al., 1995; Itazawa et al., 1997; Zhou and Hablitz, 1998; Yin et al., 1999). We have demonstrated that this deficiency also applies to synaptic AMPARs of principal neurons during early development before postnatal day 16. Our conclusions are based on the observations that (1) the *I–V* relationships of the isolated AMPAR component reveal clear differences in rectification properties between the two age groups considered; and (2) the blocking effects of either intracellular or extracellular NHPP-spermine (Kamboj et al., 1995; Mahanty and Sah, 1998; Rozov and Burnashev, 1999) and permeability to Ca^{2+} are seen only in pyramidal neurons from animals belonging to the younger age group. Because polyamine interaction with AMPARs has been observed solely in the absence of the GluR2 subunit, this suggests that changes in rectification noted above are most likely mediated through alterations in synaptic receptors. The results from experiments using dual stimulation paradigms and analysis of spontaneously occurring EPSCs further suggest that the functional properties of synaptically expressed AMPARs are not input-specific (Kumar and Huguenard, 2001).

To what extent do these changes reflect GluR2 stoichiometry of synaptic AMPARs? Washburn et al. (1997) argued that the findings of highly variable rectification and the polyamine block observed among different cells are inconsistent with a fixed stoichiometry for either recombinant or native AMPARs. Instead, the number of GluR2 subunits in individual AMPARs can vary widely. The number of GluR2 subunits in a receptor thus appears to be the primary factor influencing the degree of rectification and polyamine sensitivity. Indeed, the variability in rectification, degree of polyamine block, and GluR2 immunoreactivity we have observed, compared with other systems or neuron types, support these conclusions and suggest a low but variable GluR2 stoichiometry for synaptic AMPARs on P13–P15 pyramidal neurons unlike P16–P21 neurons.

Technical considerations

Changes in *I–V* relationships might result from age-dependent differences in the inability to adequately voltage clamp electrotonically remote synapses. We found that AMPA and NMDA receptor-mediated components of the EPSC both reversed polarity at the expected reversal potential (0 mV) in both age groups. This would not be expected if voltage-clamp reliability was compromised, as might occur, for example, with alterations in K^{+} channel expression. Furthermore, holding currents at various membrane potentials for neurons in both age groups were similar, suggesting minimal contribution of voltage-clamp errors to the observed rectification. Series resistance and rise times were also similar. These facts, together with the differential effects of intracellular spermine on AMPAR-mediated synaptic responses in the two age groups, make the above possibility unlikely.

The relatively slow rise time for AMPAR-mediated responses (cf. Geiger et al., 1997; Zhou and Hablitz, 1997) observed in our experiments is probably attributable to the remote electrotonic location of the synapses on distal dendritic spines. By contrast, spontaneous EPSCs were routinely obtained with rise times of <1 msec, indicating that the clamp–response time was adequate to obtain such measurements (Kumar and Huguenard, 2001). The rise times observed for neocortical layer 5 pyramidal neurons in this study are comparable with those obtained for CA1 synapses in the hippocampus (Hestrin et al., 1990). Although the precise locus of callosal input onto pyramidal cells in rats remains unknown, in rabbits it is restricted exclusively to the oblique branches of the apical dendrites in the adult animals, suggesting a distinct anatomical locus for the bulk of the callosal input onto these neurons (Globus and Scheibel, 1967). These synapses were localized to the deep layers 3 and 4 ~200 μm from the cell soma, which would correspond to a passive attenuation factor of ~20% (Häusser and Roth, 1997). Using a simulation approach, we find that given the equivalent series resistances and holding currents observed in young and old neurons (Fig. 3*F*), changes in neuronal morphology or leak conductance would not contribute to the observed differences in rectification (J. R. Huguenard and S. S. Kumar, unpublished observations), indicating that the developmental alterations in EPSC properties result predominantly from changes in synaptic AMPARs.

In the local perfusion experiments used for assessing Ca^{2+} permeability (Fig. 5), we found that it was necessary to increase stimulus intensity to restore synaptic responses when $[Ca^{2+}]_o$ was elevated (Otis et al., 1995). The higher stimulus intensity could potentially result in activation or recruitment of a different set of synapses or both. This seems unlikely, given the comparable waveforms and kinetics of EPSCs evoked under these conditions (Fig. 5*B*). Furthermore, experiments involving dual stimulation (intracortical and callosal; Figs. 1*F*, 4*B*) suggest that AMPAR-mediated synapses on pyramidal neurons have similar properties. Thus, increasing stimulus intensity most likely evokes a response that is dependent on the same compliment of glutamate receptors as before (note that NBQX blocks the EPSCs in elevated Ca^{2+}; Fig. 5*B*).

Interpreting anatomical results

Despite the fact that anatomical experiments provide only an indirect measure of synaptic GluR2 expression in the cells of interest, they do show that the pyramidal neurons sampled in our study change their overall phenotype from one of relatively low expression at times before ~P16 to one of high expression later in development. These results are consistent with the developmental profile of GluR2 gene expression in cortical tissue (Pellegrini-Giampietro et al., 1992). Differences in GluR2 expression between the age groups are manifested not only in terms of absolute levels within respective cells but also relative to other subunits, GluR1 and GluR4, that are coexpressed with GluR2. The fact that GluR2/1 and GluR2/4 ratio estimates in P21 neurons are larger by ~30 and 14%, respectively, compared with P12 neurons, suggests that developmental increases in GluR2 expression are

not merely attributable to increases in the total number of AMPARs expressed by these neurons but are also attributable to alterations in receptor stoichiometry.

Heterogeneity of AMPARs within single neurons

The direct demonstration that synaptic AMPARs from the younger but not the older age group are permeable to Ca^{2+} strongly supports the hypothesis of a developmentally regulated change in the subunit composition of these receptors with respect to the GluR2 subunit. Exceptions most likely include extrasynaptic AMPARs, located on the somas of neocortical pyramidal neurons, which might differ from their counterparts at the synapse in terms of their function and respective subunit compositions (Lerma et al., 1994; Carder, 1997; Yin et al., 1999). Indeed, application of glutamate to outside-out patches from pyramidal cell somas in P16 or younger neurons shifted the E_{rev} of AMPAR-mediated responses from ~0 mV in 1.8 mM Ca^{2+} to −62 mV in 100 mM Ca^{2+}, corresponding to a P_{Ca}/P_{Na} ratio of 0.04. Together with the current results, this suggests a significantly lower Ca^{2+} permeability for somatic as opposed to synaptic AMPARs (Kumar and Huguenard, 2001). The finding of input-specific AMPAR responses in hippocampal interneurons (Toth and McBain, 1998) provides further support for inhomogeneous AMPAR distribution in the neuronal somatodendritic membranes.

The GluR2 subunit and neuronal development

Previous studies have suggested that developmental regulation of Ca^{2+}-permeable AMPARs, possibly through regulation of GluR2 expression, occurs in a variety of systems. For example, in spinal interneurons of *Xenopus* embryos, there is a transient occurrence of Ca^{2+}-permeable AMPARs early in development (Rohrbough and Spitzer, 1999), as would be expected for GluR2-deficient receptors. In avian cochlear nuclei, there is an increase in sensitivity to intracellular spermine that occurs between embryonic day 11 (E11) and E18 (Lawrence and Trussell, 2000), consistent with a downregulation of GluR2 during this period. Functional GluR2 changes in synaptic receptors have not been reported previously, although colocalization studies of synaptophysin and GluR2 immunoreactivities in cultured hippocampal neurons suggest that the relative abundance of GluR2 at synaptic AMPARs increases with development (Pickard et al., 2000). Yuste et al. (1999) have also reported, using two-photon imaging with Ca^{2+} indicator dyes, that a minor subpopulation of dendritic spines on hippocampal CA1 pyramidal neurons show an APV-resistant Ca^{2+} influx with synaptic stimulation in P20 rats. These studies, including our direct demonstration of altered Ca^{2+} permeability in synaptic AMPARs, suggest that regulation of Ca^{2+} permeability in AMPARs via alterations in GluR2 content may be a common feature of neuronal development.

Functional significance

Alteration of the synaptic AMPAR subunit composition represents a novel Ca^{2+}-dependent mechanism for the control of neocortical excitability and development. The switch in GluR2 expression and the resulting change in the permeability of Ca^{2+} through these receptors (Geiger et al., 1995; Jonas and Burnashev, 1995; Gu et al., 1996; Washburn et al., 1997; Yin et al., 1999) are likely to have important functional implications relating developmental (Rohrbough and Spitzer, 1999; Lawrence and Trussell, 2000) and activity-dependent forms of synaptic plasticity (Mahanty and Sah, 1998; Liu and Cull-Candy, 2000) in the neocortex. Furthermore, the early low expression of GluR2 might underlie the increased seizure susceptibility of the immature brain (Schwartzkroin and Prince, 1980; Moshe et al., 1983; Sensi et al., 1999). In a recent study, Sanchez et al. (2001) showed that hypoxia-induced seizures in neonatal rats (P10–P12) are linked with maturational and seizure-induced changes in AMPAR composition and function, particularly in relation to the GluR2 subunit. Their results indicated further that seizures induce an increased expression of Ca^{2+}-permeable AMPARs and an increased capacity for AMPAR-mediated epileptogenesis. The AMPAR switch described in this study occurs approximately midway during the period of maximum synaptogenesis in rats (P11–P20; Sutor and Luhmann, 1995) and results in changes in the functional properties of AMPARs that depend on the presence or absence of GluR2. Failure to switch the subunit composition of these receptors to incorporate GluR2 at this juncture might have deleterious consequences relating to neocortical excitability (Pellegrini-Giampietro et al., 1997; Feldmeyer et al., 1999).

REFERENCES

Aamodt SM, Constantine-Paton M (1999) The role of neural activity in synaptic development and its implications for adult brain function. Adv Neurol 79:133–144.

Ammann D, Bissig R, Guggi M, Pretsch E, Simon W, Borowitz IJ, Weiss L (1975) Preparations of neutral ionophores for alkali and alkaline earth metal cations and their application in ion selective membrane electrodes. Helv Chim Acta 58:1535–1548.

Angulo MC, Lambolez B, Audinat E, Hestrin S, Rossier J (1997) Subunit composition, kinetic, and permeation properties of AMPA receptors in single neocortical nonpyramidal cell. J Neurosci 17:6685–6696.

Bahn S, Volk B, Wisden W (1994) Kainate receptor gene expression in the developing rat brain. J Neurosci 14:5525–5547.

Bahring R, Bowie D, Benveniste M, Mayer ML (1997) Permeation and block of rat GluR6 glutamate receptor channels by internal and external polyamines. J Physiol (Lond) 502:575–589.

Bowie D, Mayer ML (1995) Inward rectification of both AMPA and kainate subtype glutamate receptors generated by polyamine-mediated ion channel block. Neuron 15:453–462.

Burnashev N, Monyer H, Seeburg PH, Sakmann B (1992) Divalent ion permeability of AMPA receptor channels is dominated by the edited form of a single subunit. Neuron 8:189–198.

Carder RK (1997) Immunocytochemical characterization of AMPA-selective glutamate receptor subunits: laminar and compartmental distribution in macaque striate cortex. J Neurosci 17:3352–3363.

Conti C, Manzoni T (1994) The neurotransmitters and postsynaptic actions of callosally projecting neurons. Behav Brain Res 64:37–53.

Dobrunz LE, Stevens CF (1997) Heterogeneity of release probability, facilitation and depletion. Neuron 18:995–1008.

Donevan SD, Rogawski MA (1995) Intracellular polyamines mediate inward rectification of Ca^{2+}-permeable alpha-amino-3-hydroxy-5-methyl-4-isoxazolepropionic acid receptors. Proc Natl Acad Sci USA 92:9298–9302.

Feldmeyer D, Kask K, Brusa R, Kornau HC, Kolhekar R, Rozov A, Burnashev N, Jensen V, Hvalby O, Sprengel R, Seeburg PH (1999) Neurological dysfunctions in mice expressing different levels of the Q/R site-unedited AMPAR subunit GluR-B. Nat Neurosci 2:57–64.

Geiger JR, Melcher T, Koh DS, Sakmann B, Seeburg PH, Jonas P, Monyer H (1995) Relative abundance of subunit mRNAs determines gating and Ca^{2+} permeability of AMPA receptors in principal neurons and interneurons in rat CNS. Neuron 15:193–204.

Geiger JR, Lubke J, Roth A, Frotscher M, Jonas P (1997) Submillisecond AMPA receptor-mediated signalling at a principal neuron-interneuron synapse. Neuron 18:1009–1023.

Gilbertson TA, Scobey R, Wilson M (1991) Permeation of calcium ions through non-NMDA glutamate channels in retinal bipolar cells. Science 251:1613–1615.

Globus A, Scheibel AB (1967) Synaptic loci on parietal cortical neurons: terminations of corpus callosum fibers. Science 156:1127–1129.

Gu JG, Albuquerque C, Lee CJ, MacDermott AB (1996) Synaptic strengthening through activation of Ca^{2+}-permeable AMPA receptors. Nature 381:793–796.

Häusser M, Roth A (1997) Estimating the time course of the excitatory synaptic conductance in neocortical pyramidal cells using a novel voltage jump method. J Neurosci 17:7606–7625.

Hestrin S, Nicoll RA, Perkel DJ, Sah P (1990) Analysis of excitatory synaptic action in pyramidal cells using whole-cell recording from rat hippocampal slices. J Physiol (Lond) 422:203–225.

Hollmann M, Heinemann S (1994) Cloned glutamate receptors. Annu Rev Nerosci 17:31–108.
Hollmann M, Hartley M, Heinemann S (1991) Ca^{2+} permeability of KA-AMPA-gated glutamate receptor channel depends on subunit composition. Science 252:851–853.
Isa T, Iino M, Itazawa S, Ozawa S (1995) Spermine mediates inward rectification of Ca(2+)-permeable AMPA receptor channels. NeuroReport 6:2045–2048.
Itazawa S, Isa T, Ozawa S (1997) Inwardly rectifying and Ca^{2+}-permeable AMPA-type glutamate receptor channels in rat neocortical neurons. J Neurophysiol 78:2592–2601.
Ivy GO, Killackey HP (1981) The ontogeny of the distribution of callosal projection neurons in the rat parietal cortex. J Comp Neurol 195:367–389.
Jacobson S, Trojanowski JQ (1974) The cells of origin of the corpus callosum in rat, cat and rhesus monkey. Brain Res 74:149–155.
Jia Z, Agopyan N, Miu P, Xiong Z, Henderson J, Gerlai R, Taverna FA, Velumian A, MacDonald J, Carlen P, Abramow-Newerly W, Roder J (1996) Enhanced LTP in mice deficient in the AMPA receptor GluR2. Neuron 17:945–956.
Jonas P, Burnashev N (1995) Molecular mechanisms controlling calcium entry through AMPA-type glutamate receptor channels. Neuron 15:987–990.
Jonas P, Sakmann B (1992) Glutamate receptor channels in isolated patches from CA1 and CA3 pyramidal cells of rat hippocampal slices. J Physiol (Lond) 455:143–171.
Jonas P, Racca C, Sakmann B, Seeburg PH, Monyer H (1994) Differences in calcium permeability of AMPA-type glutamate receptor channels in neocortical neurons caused by differential GluR-B subunit expression. Neuron 12:1281–1289.
Kamboj SK, Swanson GT, Cull-Candy SG (1995) Intracellular spermine confers rectification on rat calcium-permeable AMPA and kainate receptors. J Physiol (Lond) 486:297–303.
Kawaguchi Y (1992) Receptor subtypes involved in callosally-induced postsynaptic potentials in rat frontal cortex in vitro. Exp Brain Res 88:33–40.
Kidd FL, Isaac TR (1999) Developmental and activity-dependent regulation of kainate receptors at thalamocortical synapses. Nature 400:569–573.
Koh DS, Burnashev N, Sakmann B (1995) Block of native Ca^{2+}-permeable AMPA receptors in rat brain by intracellular polyamines generates double rectification. J Physiol (Lond) 486:383–402.
Kumar SS, Huguenard JR (2001) Properties of excitatory synaptic connections mediated by the corpus callosum in the developing rat neocortex. J Neurophysiol 86:2973–2985.
Lawrence JJ, Trussell LO (2000) Long-term specification of AMPA receptor properties after synapse formation. J Neurosci 20:4864–4870.
Lerma J, Morales M, Ibarz JM, Somohano F (1994) Rectification properties and Ca^{2+} permeability of glutamate receptor channels in hippocampal cells. Eur J Neurosci 6:1080–1088.
Liu SQ, Cull-Candy SG (2000) Synaptic activity at calcium-permeable AMPA receptors induces a switch in receptor subtype. Nature 405:454–458.
Mahanty NK, Sah P (1998) Calcium permeable AMPA receptors mediate long-term potentiation in interneurons in the amygdala. Nature 394:683–687.
Malenka RC, Kauer JA, Perkel DJ, Nicoll RA (1989) The impact of postsynaptic calcium on synaptic transmission—its role in long-term potentiation. Trends Neurosci 12:444–450.
Mayer ML, Westbrook GL (1987) Permeation and block of *N*-methyl-D-aspartic acid receptor channels by divalent cations in mouse cultured central neurones. J Physiol (Lond) 394:501–527.
McBain CJ, Dingledine R (1993) Heterogeneity of synaptic glutamate receptors on CA3 stratum radiatum interneurones of rat hippocampus. J Physiol (Lond) 462:373–392.
Moshe SL, Albala BJ, Ackermann RF, Engel Jr J (1983) Increased seizure susceptibility of the immature brain. Dev Brain Res 7:81–85.
Otis TS, Raman IM, Trussell LO (1995) AMPA receptors with high Ca^{2+} permeability mediate synaptic transmission in the avian auditory pathway. J Physiol (Lond) 482:309–315.
Pandya DN, Seltzer B (1986) Two hemispheres-one brain: functions of the corpus callosum (Lepore F, Ptito M, Jasper HH, eds). New York: Liss.
Paxinos G, Watson C (1986) The rat brain in stereotaxic coordinates, Ed 2. San Diego: Academic.
Pellegrini-Giampietro DE, Bennett MVL, Zukin RS (1992) Are Ca^{2+}-permeable Kainate/AMPA receptors more abundant in immature brain? Neurosci Lett 144:65–69.
Pellegrini-Giampietro DE, Gorter JA, Bennett MVL, Zukin RS (1997) The GluR2 (GluR-B) hypothesis: Ca^{2+}-permeable AMPA receptors in neurological disorders. Trends Neurosci 20:464–470.
Pickard L, Noel J, Henley JM, Collingridge GL, Molnar E (2000) Developmental changes in synaptic AMPA and NMDA receptor distribution and AMPA receptor subunit composition in living hippocampal neurons. J Neurosci 20:7922–7931.
Pitzer KS, Mayorga G (1973) Thermodynamics of electrolytes. II. Activity and osmotic coefficients for strong electrolytes with one or both ions univalent. J Phys Chem 77:2300–2308.
Prince DA, Connors BW (1984) Mechanisms of epileptogenesis in cortical structures. Ann Neurol 16:59–64.
Rohrbough J, Spitzer NC (1999) Ca^{2+}-permeable AMPA receptors and spontaneous presynaptic transmitter release at developing excitatory spinal synapses. J Neurosci 19:8528–8541.
Rozov A, Burnashev N (1999) Polyamine-dependent facilitation of postsynaptic AMPA receptors counteracts paired-pulse depression. Nature 401:594–598.
Sanchez RM, Koh S, Rio C, Wang C, Lamperti ED, Sharma D, Corfas G, Jensen FE (2001) Decreased glutamate receptor 2 expression and enhanced epileptogenesis in immature rat hippocampus after perinatal hypoxia-induced seizures. J Neurosci 21:8154–8163.
Schwartzkroin PA (1995) Pathophysiology of cortical synapses and circuits. In: The cortical neuron (Gutnick MJ, Mody I, eds), pp 276–292. New York: Oxford UP.
Schwartzkroin PA, Prince DA (1980) Changes in excitatory and inhibitory synaptic potentials leading to epileptogenic activity. Brain Res 183:61–76.
Sensi SL, Yin HZ, Carriedo SG, Weiss JH (1999) Preferential zinc influx through calcium permeable AMPA/Kainate channels triggers prolonged mitochondrial superoxide production. Proc Natl Acad Sci USA 96:2414–2419.
Sutor B, Luhmann HJ (1995) Development of excitatory and inhibitory postsynaptic potentials in the rat neocortex. Perspect Dev Neurobiol 2:409–419.
Swann JW, Smith KL, Brady RJ, Pierson MG (1993) Neurophysiological studies of alterations in seizure susceptibility during development. In: Epilepsy: models, mechanisms and concepts (Schwartzkroin PA, ed), pp 209–243. Cambridge, UK: Cambridge UP.
Toth K, McBain CJ (1998) Afferent-specific innervation of two distinct AMPA receptor subtypes on single hippocampal interneurons. Nat Neurosci 1:572–578.
Vissavajjhala P, Janssen WG, Hu Y, Gazzaley AH, Moran T, Hof PR, Morrison JH (1996) Synaptic distribution of the AMPA-GluR2 subunit and its colocalization with calcium-binding proteins in rat cerebral cortex: an immunohistochemical study using a GluR2-specific monoclonal antibody. Exp Neurol 142:296–312.
Vogt BA, Gorman ALF (1982) Responses of cortical neurons to stimulation of corpus callosum in vitro. J Neurophysiol 48:1257–1273.
Washburn MS, Dingledine R (1996) Block of α-amino-3-hydroxy-5-methyl-4-isoxazolepropionic acid (AMPA) receptors by polyamines and polyamine toxins. J Pharmacol Exp Ther 278:669–678.
Washburn MS, Numberger M, Zhang S, Dingledine R (1997) Differential dependence on GluR2 expression of three characteristic features of AMPA receptors. J Neurosci 17:9393–9406.
Yin HZ, Sensi SL, Carriedo SG, Weiss JH (1999) Dendritic localization of Ca^{2+} permeable AMPA/kainate channels in hippocampal pyramidal neurons. J Comp Neurol 409:250–260.
Yuste R, Majewska A, Cash SS, Denk W (1999) Mechanisms of calcium influx into hippocampal spines: heterogeneity among spines, coincidence detection by NMDA receptors, and optical quantal analysis. J Neurosci 19:1976–1987.
Zhou F-M, Hablitz JJ (1997) Rapid kinetics and inward rectification of miniature EPSCs in layer I neurons of rat neocortex. J Neurophysiol 77:2416–2426.
Zhou F-M, Hablitz JJ (1998) AMPA receptor-mediated EPSCs in rat neocortical layer II/III interneurons have rapid kinetics. Brain Res 780:166–169.